Conference Pre-Print

Average Magnetic Drift Models for Ion Temperature Gradient Driven Instability in Tokamaks

B. Jia, Q. Zhong, and Y. Xiao*
Institute for Fusion Theory and Simulation, School of Physics, Zhejiang University, Hangzhou, People's Republic of China

Y. Li
School of Science, Tianjin University of Technology and Education, Tianjin, People's Republic of China

The ion temperature gradient (ITG) mode has long been recognized as a major driver of anomalous ion transport. Developing a reduced model that accurately incorporates kinetic effects under experimental conditions is therefore essential for understanding the underlying physics of ITG. We propose a refined constant-drift approximation based on averaging the drift frequency over the region of unfavorable curvature. Using the averaged-drift model together with a newly developed finite Larmor radius (FLR) expansion algorithm, we derive a reduced kinetic equation for ITG instabilities. When retaining only first-order FLR effects, this equation reduces to a Schrödinger-type differential equation. Extending the model via generalized translational invariance enables its successful application to the reversed magnetic shear configuration. Results from this generalized model show qualitative agreement with global gyrokinetic GTC simulations.

I. INTRODUCTION

It is well established that the ITG instability is the major driver of anomalous ion transport in Tokamaks[1]. The subsequent discovery of the internal transport barrier (ITB), characterized by steep temperature and density gradients near a magnetic shear reversal point[2], has directed significant attention toward analyzing ITG modes within reversed magnetic shear configurations. The formation of the ITB has been observed across various Tokamaks, including JT-60U[3], JET[4], TFTR[5], and DIII-D[4, 6, 7]. These observations suggest that the reversed shear region acts as an isolation layer between the enhanced confinement region inside and the region of poorer confinement outside. Therefore, a comprehensive understanding of ITG modes in reversed magnetic shear cases is essential.

Numerous numerical studies have focused on the ITG turbulence transport in reversed magnetic shear (RMS) configurations[8–10]. These works demonstrate several distinct behaviors induced by the characteristic structures of the RMS profile. Notably, radial even and odd parity eigenstates with comparable growth rates have been observed in both one-dimensional (1D) models[8, 9] and global simulations[10]. This is a significant departure from normal shear cases, where the even parity ITG mode typically exhibits a greater growth rate than the odd parity mode. The 1D slab models have shown that these mode structure characteristics are induced by the special potential structures inherent to RMS[9]. Furthermore, these studies revealed that the even and odd parity modes may merge with each other when the mode peaks, located at different radial positions, are far separated[8]. A key limitation of these 1D slab geometry models is that the magnetic drift induced by toroidal effects in Tokamaks is ignored, which precludes quantitative comparison between these 1D results and global simulations.

The primary difficulties in formulating a 1D ITG model for the RMS case arise from the invalidation of the standard ballooning mode representation and the breakdown of translational invariance. This problem has typically been addressed in two ways: either by treating the variation of the safety factor (q) profile as a second-order effect that acts on the structure of a slowly varying envelope[10, 11], or by treating the q-profile variation as a first-order effect using the generalized ballooning mode representation[12]. The latter method relies on the strong influence of the parallel mode structure on modes such as ITG, allowing the effect of the q profile to be distinguished from other global effects like density and temperature profiles. However, the poloidal dependence of the magnetic drift prevents the straightforward implementation of a 1D kinetic toroidal ITG model utilizing the generalized ballooning mode representation, thereby limiting the extension of slab models[8] to toroidal configurations. Recently, the average magnetic drift approximation has been shown to provide a reasonable ITG model in the Schrödinger form[13]. This model demonstrates consistency with global gyrokinetic simulation results from GTC[14], and highlights the significant role of the average magnetic drift frequency (induced by the toroidal effect) in the linear dispersion relation of ITG. By assuming that the magnetic drift frequency is independent of the poloidal angle, this approximation allows us to extend the existing slab ITG model[8] to a toroidal case that incorporates the essential magnetic drift effects. This paper focuses on the derivation and implementation

* yxiao@zju.edu.cn

of this extended model.

II. REDUCED KINETIC MODEL

We start from the ITG eigenvalue equation in ballooning space. Perturbed particle density δn_j in the gyrokinetic theory[15] can be decomposed into adiabatic and nonadiabatic components in the form of

$$\delta n_j = -n_{0j}\frac{q_j\delta\phi}{T_j} + n_{0j}\int d\boldsymbol{v} h_j J_0\left[k_\perp\left(\eta\right)\alpha_j\right], \quad (1)$$

where the subscript j represents particle species ($j = i$ for ion, $j = e$ for electron), $q_e = -e, q_i = Z_i e$ ($Z_i = 1$ throughout this paper), $\delta\phi$ is perturbed electrostatic potential, n_{0j} is unperturbed density, T_j is temperature, $\alpha_j = v_\perp/\Omega_j$ is gyroradius with gyrofrequency $\Omega_j = q_j B/m_j$, $k_\perp = k_\theta\sqrt{1+\hat{s}^2\eta^2}$ is the wave vector perpendicular to the field line with η, $\hat{s}$, k_θ representing the extended poloidal angle, magnetic shear and poloidal wave number, respectively, and the zeroth order Bessel function J_0 comes from the finite Larmor radius (FLR) effects. While electron is assumed adiabatic such that the non-adiabatic perturbed electron gyrocenter distribution $h_e = 0$, the non-adiabatic perturbed ion gyrocenter distribution h_i is given by solving the gyrokinetic equation[15, 16]

$$\left(i\frac{v_\parallel}{qR}\frac{\partial}{\partial\eta} + \omega - \omega_{di}\right)h_i = \frac{q_i F_{Mi}}{T_i}\left(\omega - \omega_{*i}^T\right)J_0\left[k_\perp\left(\eta\right)\alpha_i\right]\delta\phi\left(\eta\right) \quad (2)$$

in which

$$\begin{aligned}
\omega_{*i}^T &= \omega_{*i}\left[1+\eta_i\left(v^2/2v_{ti}^2 - 3/2\right)\right]\\
\omega_{*i} &= T_i/m_i\Omega_i\boldsymbol{k}\times\boldsymbol{b}\cdot\nabla\ln n_{0i}\\
\omega_{di} &= \bar{\omega}_{di}\left[\cos\left(\eta\right)+\hat{s}\eta\sin\left(\eta\right)\right]\left(v_\parallel^2 + v_\perp^2/2\right)/2v_{ti}^2\\
F_{Mi} &= \left(2\pi v_{ti}^2\right)^{-\frac{3}{2}}\exp\left(-v^2/2v_{ti}^2\right)\\
\eta_i &= d\ln T_i/d\ln n_{0i}
\end{aligned}$$

with q, m_i and $v_{ti} = \sqrt{T_i/m_i}$ representing the safety factor, ion mass and ion thermal velocity, respectively. By substituting the density perturbations of ion and electron into the quasineutrality condition, the linear ITG eigen problem is formulated as:

$$\left(1+\frac{1}{\tau}\right)\delta\phi\left(\eta\right) = \int_{-\infty}^{\infty} d\eta' K\left(\omega,\eta,\eta'\right)\delta\phi\left(\eta'\right), \quad (3)$$

where $\tau = T_e/T_i$ and K is the velocity space integration of the non-adiabatic response[13, 16–19]. It's found that Eq. (3) can be simplified by the average magnetic drift approximation[13]

$$\omega_d \approx \bar{\omega}_{dj} f\left(\hat{s}\right)\frac{v_\parallel^2 + v_\perp^2/2}{2v_{tj}^2}, \quad (4)$$

$$f\left(\hat{s}\right) = \left\langle\cos\left(\eta\right)+\hat{s}\eta\sin\left(\eta\right)\right\rangle_{-\eta_s}^{\eta_s}, \quad (5)$$

where operator $\langle\rangle_{-\eta_s}^{\eta_s}$ means average over the bad curvature region $\eta\in[-\eta_s,\eta_s]$ with η_s determined by equation $\cos\left(\eta_s\right)+\hat{s}\eta_s\sin\left(\eta_s\right) = 0$. Under the average magnetic drift approximation, the gyrokinetic equation Eq. (2) reduces to a first-order, linear ordinary differential equation with constant coefficients. It then can be transformed to the Fourier space (radial space, $z = qRk_\parallel$ is the Fourier conjugation of η) taking the form

$$\begin{aligned}
&\left(-\frac{v_\parallel}{qR}z+\omega\right)\hat{h}_j\left(z\right) - \bar{\omega}_{dj} f\left(\hat{s}\right)\frac{v_\parallel^2+v_\perp^2/2}{2v_{tj}^2}\hat{h_j}\left(z\right) \quad (6)\\
&= \frac{q_j F_{Mj}}{T_j}\left(\omega-\omega_{*j}^T\right)\mathcal{F}\left\{J_0\left[k_\perp\left(\eta\right)\alpha_j\right]\delta\phi\left(\eta\right)\right\}.
\end{aligned}$$

With the first-order FLR expansion

$$\begin{aligned}
&J_0^2\left(\sqrt{2b}x_\perp\right) \approx J_0^2\left(\sqrt{2b_\theta}x_\perp\right) \quad (7)\\
&- J_0\left(\sqrt{2b_\theta}x_\perp\right)J_1\left(\sqrt{2b_\theta}x_\perp\right)\sqrt{\frac{2}{b_\theta}}x_\perp\left(-b_\theta\hat{s}^2\frac{\partial^2}{\partial z^2}\right), \quad (8)
\end{aligned}$$

The radial ITG eigenvalue problem[13, 20] can be formulated as:

$$\left\{\frac{\partial^2}{\partial z^2} + \frac{\bar{\omega}_{di} f\left(\hat{s}\right)\left(1+\frac{1}{\tau}\right)+\mathcal{K}_0}{\sqrt{2b_\theta}\hat{s}^2\mathcal{K}_1}\right\}\delta\phi\left(z\right) = 0, \quad (9)$$

where the integrals $\mathcal{K}_0$ and $\mathcal{K}_1$ are related to the velocity integrations which are defined as:

$$\mathcal{K}_0 = \left[\omega-\omega_{*i}\left(1-\frac{3}{2}\eta_i\right)\right]\mathcal{M}_{10} - \eta_i\omega_{*i}\left(\mathcal{M}_{30}+\mathcal{M}_{12}\right), \quad (10)$$

$$\mathcal{K}_1 = \left[\omega-\omega_{*i}\left(1-\frac{3}{2}\eta_i\right)\right]\mathcal{N}_{20} - \eta_i\omega_{*i}\left(\mathcal{N}_{40}+\mathcal{N}_{22}\right), \quad (11)$$

where $\mathcal{M}_{(n,m)}$ and $\mathcal{N}_{(n,m)}$ denote the two-dimensional velocity quadratures which can be solved by the generalized plasma dispersion function[21, 22].

III. REDUCED KINETIC MODEL IN REVERSED SHEAR CASE

The preceding model, constructed in the ballooning space, rely on the assumption of the translational invariance[23]. However, this assumption is invalid in a reversed magnetic shear configuration, which breaks the translational invariance and causes the standard ballooning mode representation to fail. In these cases, the generalized ballooning mode representation[12] or generalized translational invariance must be employed. For simplicity, we assume that q profile is in quadratic form[12, 24]

$$q = q_0 + \frac{\delta_{A,m}}{n} + q_0\hat{s}\frac{\left(r-r_0\right)}{r_0} + \frac{q_0^2 s_2^2}{2}\frac{\left(r-r_0\right)^2}{r_0^2},$$

where

$$\hat{s} = \frac{r_0 q'(r_0)}{q_0},\ s_2^2 = \frac{q'' r_0^2}{q_0^2},\ q_0 = \frac{m}{n}, \tag{12}$$

and r_0 is the reference flux surface. Therefore,

$$nq - m = \delta_{A,m} + \hat{s} r_\kappa + \frac{s_2^2}{2n} r_\kappa^2 = q_0 R_0 k_\parallel, \tag{13}$$

where $r_\kappa = k_\theta (r - r_0)$. The parameter $\delta_{A,m} = n(q(r_0) - q_0)$ quantifies the deviation of the safety factor q at the reference flux surface (r_0) from the rational number q_0. For the reversed shear case considered in this paper, where we set $\hat{s} = 0$ and $s_2^2/2n > 0$, the number of rational surfaces is determined by $\delta_{A,m}$: two for $\delta_{A,m} < 0$, one for $\delta_{A,m} = 0$, and none for $\delta_{A,m} > 0$. n and s_2 can be considered as a single parameter since they only appear in the form $s_2^2/2n$, However, we choose to keep parameter $n = 10$ hereafter for the convenience of comparison with GTC. Furthermore, Eq. (13) reduce to normal shear case conveniently when $s_2 = 0$, which allows the normal and reversed magnetic shear cases to be considered uniformly using the above expressions.

The reduced magnetic drift model for reversed magnetic shear is analogous to that for normal shear. We adopt the average magnetic drift model given by:

$$\omega_d = \bar{\omega}_{di} f(0) \frac{v_\parallel^2 + v_\perp^2/2}{2 v_{tj}^2}. \tag{14}$$

This formulation allows the eigenvalue equation for ITG modes to be represented in the r_κ space. The radial eigenvalue equation can then be written as:

$$\left(\frac{\partial^2}{\partial r_\kappa^2} + \frac{\bar{\omega}_{di} f(\hat{s}) \left(1 + \frac{1}{\tau}\right) + \mathcal{K}_0}{\sqrt{2 b_\theta} \mathcal{K}_1} \right) \delta\phi(r_\kappa) = 0. \tag{15}$$

To verify the validity of the simplified model Eq. (15), the CBC parameters were modified for a reversed shear scenario. The equilibrium is defined by the parameters $\eta_i = 3.13$, $\epsilon_n = 0.45$, $\tau = 1$, $n = 10$, $k_\theta \rho_i = 0.4$ and a q-profile given by

$$q(\psi_n) = 2.0 - 3.1\psi_n + 4.0\psi_n^2,$$

This profile reverses at $\psi_n = 0.39$, where the safety factor is $q = 1.4$. Assuming a linear relationship between ψ_n and the radial coordinate r_κ, the q-profile can be described by a quadratic function of r_κ in the form:

$$q = q_0 + \frac{1}{n}\left(\delta_{A,m} + \hat{s} r_\kappa + \frac{s_2^2}{2n} r_\kappa^2\right),$$

with parameters set to $\delta_{A,m} = 0$, $\hat{s} = 0$, $s_2 = 1.78$ (these parameter settings are hereafter referred to as the reversed magnetic shear CBC parameters). The verification proceeds in two steps. First, the convergence of the FLR expansion is assessed by plotting the dispersion relations for different FLR expansion orders, as shown in Fig. (1) (a). These results demonstrate excellent convergence. Next, a comparison is made between the first-order simplified equation Eq. (15) and GTC simulation results, depicted in Fig. (1) (b). The results show good agreements, with some acceptable discrepancies observed at large $k_\theta \rho_i$, which confirms the validity of the simplified model Eq. (15) for the reversed shear case.

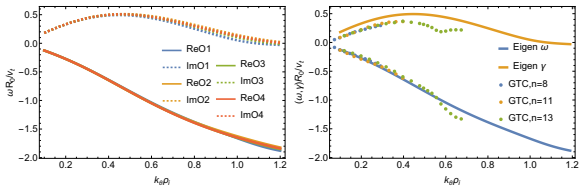

(a) (b)

Figure 1: Dispersion relations derived from the reduced model and compared with GTC simulation results. (a) Real frequency (solid lines) and growth rate (dashed lines) of the dispersion relation calculated using the first four orders of the Finite Larmor Radius (FLR) expansion (blue, orange, green, and red lines, respectively). (b) Comparison between the first-order FLR expansion and GTC simulation results. The first-order FLR expansion real frequency and growth rate are shown by the blue and orange solid lines, respectively. The GTC results for different toroidal mode numbers (n) are represented by blue, orange, and green solid markers.

IV. SUMMARY

This work successfully presented a reduced kinetic model for the ITG mode in toroidal configurations, which is applicable to both normal and RMS cases. The model is built upon the concepts of translational invariance and its extension, generalized translational invariance. Through quantitative comparison with GTC results, we demonstrated that the reduced kinetic model is reliable across relevant experimental parameters.

[1] L. Chen, S. Briguglio, and F. Romanelli. The long-wavelength limit of the ion-temperature gradient mode in tokamak plasmas. *Physics of Fluids B: Plasma Physics*, 3:611–614, 3 1991.

[2] J. Q. Dong, Y. Z. Zhang, and S. M. Mahajan. Studies of instability and transport in sheared-slab plasmas with very weak magnetic shear. *Physics of Plasmas*, 4(9):3334–3340, 09 1997.

[3] Y Koide, M Kikuchi, M Mori, S Tsuji, S Ishida, N Asakura, Y Kamada, T Nishitani, Y Kawano, T Hatae, T Fujita, T Fukuda, A Sakasai, T Kondoh, R Yoshino, and Y Neyatani. Internal transport barrier on q =3 surface and poloidal plasma spin up in jt-60u high-p discharges spontaneous formation of an internal transport barrier was observed associated with improved confinement in the high-p discharges in the jt-60u tokamak. the radial location of the transport bar. 1993.

[4] C. Kessel, J. Manickam, G. Rewoldt, and W. M. Tang. Improved plasma performance in tokamaks with negative magnetic shear. *Physical Review Letters*, 72:1212, 2 1994.

[5] F M Levinton, M C Zarnstorff, S H Batha, ' M Bell, R E Bell, R V Budny, C Bush, Z Chang, E Fredrickson, A Janos, J Manickam, A Ramsey, S A Sabbagh, G L Schmidt, E J Synakowski, and G Taylor. Improved confinement with reversed magnetic shear in tftr. *NUMBER 24 PHYSICAL REVIEW LETTERS*, 75.

[6] L. L. Lao, K. H. Burrell, T. S. Casper, V. S. Chan, M. S. Chu, J. C. Deboo, E. J. Doyle, R. D. Durst, C. B. Forest, C. M. Greenfield, R. J. Groebner, F. L. Hinton, Y. Kawano, E. A. Lazarus, Y. R. Lin-liu, M. E. Mauel, W. H. Meyer, R. L. Miller, G. A. Navratil, T. H. Osborne, Q. Peng, C. L. Rettig, G. Rewoldt, T. L. Rhodes, B. W. Rice, D. P. Schissel, B. W. Stallard, E. J. Strait, W. M. Tang, T. S. Taylor, A. D. Turnbull, and R. E. Waltz. Rotational and magnetic shear stabilization of magnetohydrodynamic modes and turbulence in diii-d high performance discharges. *Physics of Plasmas*, 3:1951–1958, 5 1996.

[7] Takaaki Fujita, S Ide, H Shirai, M Kikuchi, O Naito, Y Koide, S Takeji, H Kubo, and S Ishida. Internal transport barrier for electrons in jt-60u reversed shear discharges. *Physical review letters*, 78(12):2377, 1997.

[8] J. Q. Dong, W. Horton, and Y. Kishimoto. Gyrokinetic study of ion temperature gradient instability in vicinity of flux surfaces with reversed magnetic shear. *Physics of Plasmas*, 8:167–173, 1 2001.

[9] Jiquan Li, Lin Huang, and Wenxiao Qu. Sheared slab η i instability in tokamak plasma with negative magnetic shear. *Physics of Plasmas*, 5(4):959–965, 1998.

[10] Y. Kishimoto, J.-Y. Kim, W. Horton, T. Tajima, M.J. LeBrun, S.A. Dettrick, J.Q. Li, and S. Shirai. Discontinuity model for internal transport barrier formation in reversed magnetic shear plasmas. *Nuclear Fusion*, 40(3Y):667, mar 2000.

[11] J. Y. Kim, Y. Kishimoto, M. Wakatani, and T. Tajima. Poloidal shear flow effect on toroidal ion temperature gradient mode: A theory and simulation. *Physics of Plasmas*, 3(10):3689–3695, 10 1996.

[12] F. Zonca, S. Briguglio, L. Chen, S. Dettrick, G. Fogaccia, D. Testa, and G. Vlad. Energetic particle mode stability in tokamaks with hollow q-profiles. *Physics of Plasmas*, 9:4939–4956, 12 2002.

[13] B. Jia, Q. Zhong, Y. Li, and Y. Xiao. Average magnetic drift models for ion temperature gradient-driven instability in tokamaks. *Physics of Plasmas*, 32(5):052104, 05 2025.

[14] Z. Lin, T. S. Hahm, W. W. Lee, W. M. Tang, and R. B. White. Turbulent transport reduction by zonal flows: Massively parallel simulations. *Science*, 281(5384):1835–1837, 1998.

[15] E. A. Frieman and Liu Chen. Nonlinear gyrokinetic equations for low-frequency electromagnetic waves in general plasma equilibria. *Physics of Fluids*, 25:502–508, 1982.

[16] J. Y. Kim, W. Horton, and J. Q. Dong. Electromagnetic effect on the toroidal ion temperature gradient mode. *Physics of Fluids B: Plasma Physics*, 5:4030–4039, 11 1993.

[17] F. Romanelli. Ion temperature-gradient-driven modes and anomalous ion transport in tokamaks. *Physics of Fluids B*, 1:1018–1025, 5 1989.

[18] J. Q. Dong, W. Horton, and J. Y. Kim. Toroidal kinetic ηi mode study in high temperature plasmas. *Physics of Fluids B: Plasma Physics*, 4(7):1867–1876, 07 1992.

[19] Hua-sheng Xie, Yueyan Li, Z. Lu, W. Ou, and Bo Li. Comparisons and applications of four independent numerical approaches for linear gyrokinetic drift modes. *Physics of Plasmas*, 24, 06 2017.

[20] L. Chen. private communication.

[21] Ö D Gürcan. Numerical computation of the modified plasma dispersion function with curvature. *Journal of Computational Physics*, 269:156–167, 2014.

[22] J. Y. Kim, Y. Kishimoto, W. Horton, and T. Tajima. Kinetic resonance damping rate of the toroidal ion temperature gradient mode. *Physics of Plasmas*, 1:927–936, 1994.

[23] Fulvio Zonca and Liu Chen. Theory of continuum damping of toroidal alfvén eigenmodes in finite- tokamaks. *Physics of Fluids B: Plasma Physics*, 5(10):3668–3690, 10 1993.

[24] J. Q. Dong, W. Horton, and Y. Kishimoto. Gyrokinetic study of ion temperature gradient instability in vicinity of flux surfaces with reversed magnetic shear. *Physics of Plasmas*, 8(1):167–173, 2001.